# Theoretical study on electron transfer in biological systems (III)

## ——Intramolecular electron transfer in metal-containing spiro π-electron system

ZHAI Yufeng (翟宇峰), JIANG Hualiang (蒋华良), ZHU Weiliang (朱维良), GU Jiande (顾健德), CHEN Jianzhong (陈建忠), CHEN Kaixian (陈凯先)* and JI Ruyun (嵇汝运)

(Shanghai Institute of Materia Medica, Chinese Academy of Sciences, Shanghai 200031, China)

Received July 9, 1998

**Abstract** Intramolecular electron transfer of metal-containing spiro π-electron system was studied by AM1 method in the MOPAC-ET program developed by the present group. The results indicated that with the increasing of the outer electric field $F$, the activation energy of the reaction decreased. When $F$ reaches a certain threshold value, the activation energy barrier becomes zero and the rate of reaction achieves the largest value. The results also indicated that electron transfer matrix elements $V_{AB}$ and reorganization energy $\lambda$ were not obviously affected by outer electric field while the exothermicity $\Delta E$ was directly proportional to it.

**Keywords:** **electron transfer, electric field, AM1 method, electron transfer matrix elements.**

Electron transfer (ET) processes are of greatly important reactions, which have been quickly developed after the availability of many radioactive isotopes and the introduction of related new instrument since the late 1940s[1]. The researches in this area have now widely deepened in ET reactions of chemistry and biology[2,3]. ET reactions widely exist in biological processes such as respiration and photosynthesis[4], of which intramolecular electron transfer plays a central role. Since electron transfer in metal containing protein is the main object of the research in this field[5], we designed a metal containing organic compound in which electron can transfer from one "end" to another, as shown in fig. 1, to simulate intramolecular ET in proteins. This molecule is separated by a rigid $\sigma$ bridge which makes the plane of the left end perpendicular to that of the right end. As shown in fig. 1, 1A represents left-localized state A, 1B represents right-localized state B. Theoretically, the system can be taken as an ET reaction precess, of which the initial state and final state are composed by state A and state B, respectively. The electron hops back and forth between state A and state B at a certain frequency, which is determined by the height and the shape of the potential barrier. The symmetry of the two potential surface will be broken when affected

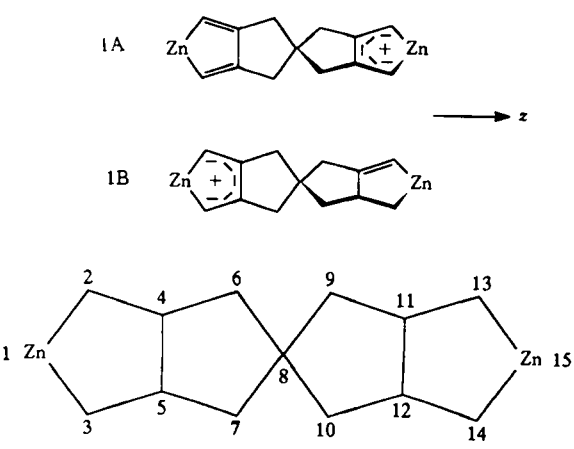


Fig. 1. Metal containing spiro-π compound and atomic ID.

by outer factors (such as an external electric field), and the activation energy will also change accordingly. Though this system is somewhat simple in simulating electron transfer in biological systems, it may release some useful information for the research in metal-containing proteins in the future. *Ab initio* method has been used to study the electron transfer[6,7]. *Ab initio* is an accurate quantum calculation method that has the predominant advantage; however, it requires expensive computational facilities such as large memory, and high CPU speed for calculation of large biology systems. With the respect of such limitation, we introduced a new function into the semi-empirical quantum chemistry program package MOPAC, and developed a new program MOPAC-ET that can be used to compute electron transfer. This program is proper for the larger molecules such as biological systems. We have compared the calculation results of *ab initio* and MOPAC-ET for a model compound, which shows the latter are reliable[8]. In this paper, we will report the calculation results for the ET process of our designed metal-containing compound with the MOPAC-ET program.

## 1 Theory and method

A lot of theoretical studies on ET reactions have been reported[9,10]. Here we only briefly introduce some simple concepts. As shown in fig. 2, the potential energy surface (PES) of the left-localized electronic state, $\Psi_A$, has a global minimum at its equilibrium nuclear configuration $Q_A$; similarly, the right-localized electronic state, $\Psi_B$, has its own global minimum configuration at $Q_B$. Obviously, $Q_A \neq Q_B$, and the two PESes cross at nuclear configuration $Q_C$. The energy difference ($\Delta E$) between the two PES minima is defined as exothermicity. According to Marcus model[6], the rate of reaction may be expressed as

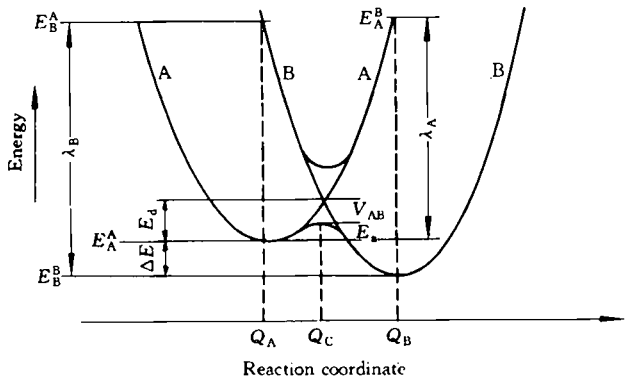


Fig. 2. Sketch map for the electron transfer (ET) reaction.

$$k_{TST} = \kappa(k_B T/h)\exp(\Delta S^{\ddagger}/k_B)\exp(-\Delta H^{\ddagger}/k_B T), \quad (1)$$

where $\kappa$ is the electronic transmission coefficient, $k_B$ is the Boltzmann's constant, $\Delta S^{\ddagger}$ and $\Delta H^{\ddagger}$ are the activation entropy and enthalpy, respectively. $\kappa$ depends on $V_{AB}$, which may be calculated by eq. (2), i.e.

$$V_{AB} = \Delta/2 = (1 - S_{AB}^2)^{-1} | H_{AB} - S_{AB}(H_{AA} + H_{BB})/2 |, \quad (2)$$

where $S_{AB} = \langle \Psi_A | \Psi_B \rangle$, $H_{AA} = \langle \Psi_A | H | \Psi_A \rangle$, $H_{BB} = \langle \Psi_B | H | \Psi_B \rangle$, and $H$ is the electronic Hamiltonian. $V_{AB}$ is an important quantity that is used in every model of electron transfer reaction. Our program encoded into MOPAC can be used to calculate this parameter. Since $\Delta S^{\ddagger}$ is sufficiently small, the activation energy $E_{act}$ is very close to $\Delta H^{\ddagger}$. There are three regions in the ET reaction according to the relative value of $\lambda$ and $\Delta E$: in the field where $\lambda > |\Delta E|$, we have what is usually referred to as the "normal" region; with the increase of $|\Delta E|$, the activation energy decreases and the rate of reaction increases, when $\lambda = |\Delta E|$, the ET process came into

"barrier free" region where the activation energy is zero and the rate of reaction reaches its maximum; if $\lambda < |\Delta E|$, the region is named "inverted region" where the activation energy will increase again. In this paper, we change the exothermicity of the reaction by applying external electric field with different strengths, and convert the reaction from the normal region to the inverted region.

All the semiempirical calculations in this paper were performed with AMl option of MOPAC-ET method. The structure of molecule A is completely optimized by using unrestricted Hatree-Fock (UHF) method with $C_{2V}$ symmetry. The structure of B is obtained from 2A frame by a 180° rotation around $y$ axis followed by a 90° rotation around $z$ axis. For the systems we studied, there are no obvious conformational change. It is, therefore, reasonable to set up the reaction coordinate $\xi$ as the linear mixture of $Q_A$ and $Q_B$, i.e. $\xi$ can be difined by eq. (3), i.e.

$$Q = \xi Q_B + (1 - \xi) Q_A, \tag{3}$$

where $Q$ is the nuclear configuration at any point on the assumed reaction path. For the symmetric molecules, the two potential surfaces are crossed at the point $\xi = 0.5$. In the calculation of $H_{AB}$, the separation of state A and state B is induced by the molecular wavefunction of $Q_A$ and $Q_B$[8].

## 2 Results and discussion

### 2.1 Geometry

The atomic ID of the stable geometries of state A and state B, and those of point at the reaction coordinate are shown in fig. 1. The geometry parameters of $Q_A(\xi = 0.0)$, $Q_B(\xi = 1.0)$ and $Q_C(\xi = 0.5)$ are listed in table 1.

Table 1 Geometries of molecule at the point where $\xi = 0.0$ ($Q_A$), $\xi = 0.5$ ($Q_C$) and $\xi = 1.0$ ($Q_B$) when the external electric field strength is zero

| | | $Q_A$ | $Q_C$ | $Q_B$ | | $Q_A$ | $Q_C$ | $Q_B$ |
|---|---|---|---|---|---|---|---|---|
| Bond length/nm | 1-2 | 0.194 | 0.195 | 0.196 | 2-4 | 0.134 | 0.137 | 0.139 |
| | 4-5 | 0.154 | 0.148 | 0.145 | 4-6 | 0.149 | 0.149 | 0.149 |
| | 6-8 | 0.154 | 0.155 | 0.155 | 8-9 | 0.155 | 0.155 | 0.154 |
| | 9-11 | 0.149 | 0.149 | 0.149 | 11-12 | 0.145 | 0.148 | 0.154 |
| | 11-13 | 0.139 | 0.137 | 0.134 | 13-15 | 0.196 | 0.195 | 0.194 |
| Bond angle/(°) | 3-1-2 | 98.53 | 96.87 | 95.22 | 1-2-4 | 98.35 | 99.78 | 101.18 |
| | 2-4-5 | 122.38 | 121.78 | 121.21 | 5-4-6 | 108.99 | 109.47 | 109.95 |
| | 4-6-8 | 107.63 | 107.45 | 107.27 | 6-8-7 | 106.75 | 106.15 | 105.55 |
| | 9-8-10 | 105.55 | 106.15 | 106.75 | 8-9-11 | 107.27 | 107.45 | 107.63 |
| | 9-11-12 | 109.95 | 109.47 | 108.99 | 12-11-13 | 121.21 | 121.78 | 122.38 |
| | 11-13-15 | 101.18 | 99.78 | 98.35 | 13-15-14 | 95.22 | 96.879 | 98.53 |

Since the heavy atoms of the left and right parts of the system are located at two perpendicular planes, and torsional angles of the system do not change too much during the ET process, the dihedral angles are not listed in table 1. According to table 1, the changes of the bond angles during the reaction are small, the maximum changes are ∠3-1-2 and ∠13-15-14, which vary between 95.219° and 98.534°. Obvious changes were found in the bonds C2—C4, C3—C5, C4—C5, C11—C13, C11—C12 and C12—C14. For example, the bond length of C2—C4 and C3—C5 change from 0.134 nm to 0.139 nm, that of C4—C5 changes from

0.154 nm to 0.145 nm. This indicated that double bonds C2═C4 and C3═C5 would be delocalized among atoms 2 to 5 when the system converted from state A to state B. Same phenomena were found among bonds C11—C13, C11—C12 and C12—C14, but the localizing-delocalizing trend is opposite, i.e. the delocalized double bonds among atoms $C_{11}$ to $C_{14}$ changed to localized double bonds C11═C13, C12═C14 and single bond C11—C12.

2.2 Total energy, exothermicity and reorganization energy

During the treatment of the title compound, we defined the spiro atom C at the origin of the coordinate and applied electric field $F$ with different strengths in the direction of $z$ axis. The trend in the changes of total energy with external electric field $F$ can be scaled by the dipole moments of state A and state B qualitatively. For state A, charge is localized in the right part of the molecule and the dipole moment is in the negative direction of axis $z$, so the energy of state A will increase with the electric field strength (the electric field is in the positive direction of $z$ axis). In the case of state B, the total energy will decrease accordingly, as shown in fig. 3, this trend will inevitably cause the crossing point $\xi_C$ to appear before 0.5; when $F$ reaches a certain value (8.29 V/nm in this article), the electron transfer reaction achieved "barrier free" region at $\xi_C = 0$ where the rate of reaction is maximal.

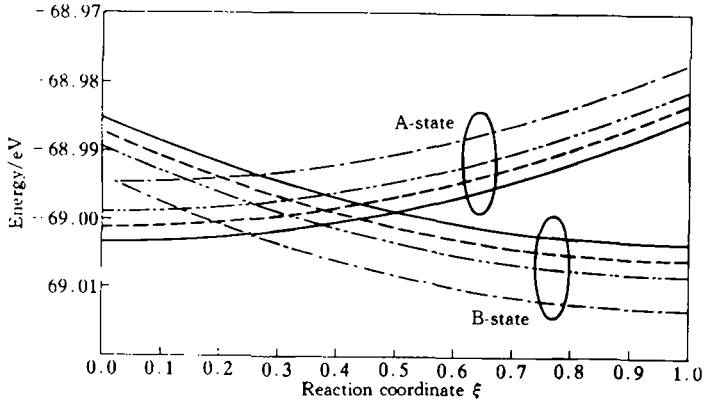


Fig. 3. Variation of the total energy (eV) versus reaction coordinate ($\xi$) under different external electric fields ($\times 10^{-1}$ V·nm$^{-1}$): ——, 0.0; - - -, 0.2; ·····, 0.4; · - · - · -, 0.8.

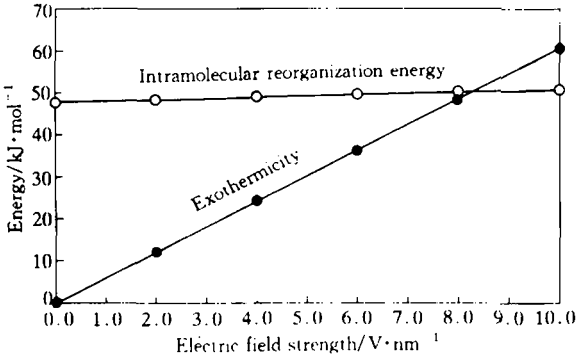


Fig. 4. Variation of reorganization energy and exothermicity versus electric field strength.

We also calculated the intramolecular reorganization energy $\lambda = E_B^A - E_B^B$ and exothermicity $|\Delta E| = E_A^A - E_B^B$ (fig. 4). The results of calculation show that with the increase of external electric field strength, the value of reorganization almost remains constant, and the exothermicity is in direct proportion to the electric field strength. For example, when the values of $F$ are 0.0, 4.0 and 8.0 V/nm respectively, those of $\lambda$ are 47.87, 49.03 and 50.16 kJ/mol, while those of $\Delta E$ are 0.0, 24.24 and 48.47 kJ/mol, respectively. When $F$ equals 8.29 V/nm, $\lambda = \Delta E$ and $\xi_C = 0$, the activation energy of the reac-

tion decreases to zero accordingly. The insensitivity of $\lambda$ to $F$ might be due to the reason that the coordinates of the configurations located in the lowest energy point in the reaction pathway cannot be changed seriously by the external electric field.

2.3 Electron transfer element $V_{AB}$

Figure 5 is the electron transfer matrix element, $V_{AB}$s, with respect to the variation of the reaction coordinates, from which we can deduce that $V_{AB}$ is insensitive to the variation of reaction coordinates, especially near the point of $Q_C$ where the two PESes crossed. In addition, $V_{AB}$ is also insensitive to the external electric field strength $F$ at reaction coordinate $\xi_C$; for example, the values are 4.212 ($\xi_C = 0.5$), 4.213 ($\xi_C = 0.259$), and 4.218 kJ/mol ($\xi_C = 0.017\ 7$) when $F$ are 0.0, 4.0 and 8.0 V/nm, respectively.

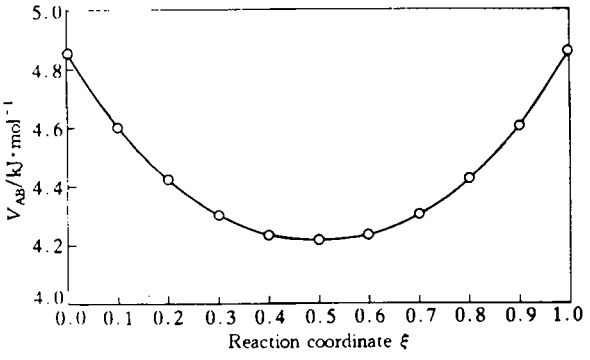


Fig. 5. Variation of $V_{AB}$ with respect to the reaction coordinate $\xi$.

2.4 Activation energy and the rate of reaction

According to eq. (1), the rate of reaction is mainly affected by $\kappa$ and $\Delta H^{\ddagger}$, in which $\Delta H^{\ddagger}$ approximately equals diabatic activation energy $E_d$. According to the Landau-Zener model[11], $\kappa$ depends on $V_{AB}$ and the slopes of the diabatic potential curves of state A and state B at the crossing seam. We have mentioned that none of these quantities changes significantly with $F$. Hence, the main contribution to the change in ET rate comes from $E_d$. Fig. 6 is the variation of the activation energy $E_d$ versus external electric field strength, from which we can see that $E_d$ has its maximum value at zero field strength and then monotonously goes to zero at the field strength of 8.29 V/nm. Fig. 6 also shows the trend of adiabatic activation energy $E_a = E_d - V_{AB}$ versus external electric field strength. In the normal region, Marcus' model is applicable and the ET rate $k_{et}(F)$ increases exponentially as a function of $F$. For instance, at room temperature, $k_{et}(0.0) : k_{et}(4.0) : k_{et}(8.29) = 1 : 38 : 123$.

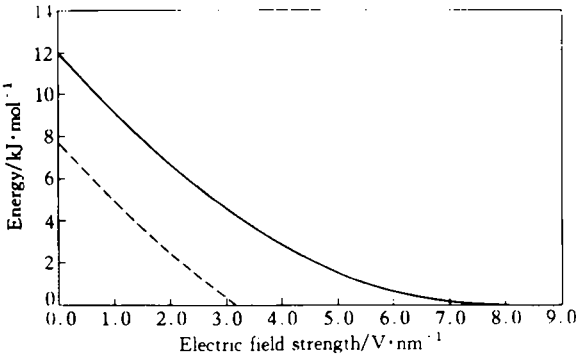


Fig. 6. Variation of the diabatic activation energy $E_d$ (——) and adiabatic activation energy $E_a$ ( - - ) (kJ/mol) versus external electric field strength.

## 3 Conclusion

In this paper, intramolecular electron transfer of the title compound is studied with AMl method in the MOPAC-ET program developed by the present group. The results show that the potential barrier of the reaction decreases with the increase of $F$, and reaches zero when $F$ is 8.29 V/nm, at this point the rate of reaction reaches maximum. Calculation also indicated that $V_{AB}$ and $\lambda$ were not obviously affected by external electric field while the $\Delta E$ values were directly

proportional to it.

## References


1 Marcus, R. A., Electron transfer reactions in chemistry: Theory and experiment (Nobel lecture), *Angew. Chem. Int.*, Eng. ed., 1993, 32(8): 1111.

2 Marcus, R. A., Sutin, N., Electron transfers in chemistry and biology, *Biochim. Biophys. Acta*, 1985, 811(3): 265.

3 Gray, H. B., Winkler, J. R., Electron transfer in proteins, *Annu. Rev. Biochem.*, 1996, 65: 537.

4 Bicout, D. J., Field, M. J., Electron transfer in proteins: A multiple scattering approach to electronic coupling, *J. Phys. Chem.*, 1995, 99(33): 12661.

5 Petterson-Kennedy, S. E., McGourty, J. L., Kalweit, J. A. et al., Temperature dependence of and ligation effects on long-range electron transfer in complementary [Ze, $Fe^{III}$] hemoglobin hybrids, *J. Am. Chem. Soc.*, 1986, 108(8): 1739.

6 Farazdel, A., Dupuis, M., Clementi, E. et al., Electric field induced intramolecular electron transfer in spiro π-electron systems and their suitability as molecular electronic devices: A theoretical study, *J. Am. Chem. Soc.*, 1990, 112(11): 4206.

7 Li, X. Y., Tian, A. M., He, F. C. et al., Electronic field dependence of the diabatic potential energy surface for gas-phase electron transfer $O_2O_2 \rightarrow O_2O_2^-$, *Chem. Phys. Lett.*, 1995, 233(3): 227.

8 Zhai, Y. F., Gu, J. D., Jiang, H. L., Theoretical study on the elctron transfer in biological system (I)——A method for calculating the electron transfer and its application to spiro π-electron system, *Acta Chimica Sinica* (in Chinese), 1998, 56 (11): 1081.

9 Dogonadze, R. R., Kuznetsov, A. M., Marsagishvili, T. A., The present state of the theory of charge transfer processes in condensed phase, *Electrochim. Acta*, 1980, 25(1): 1.

10 Newton, M. D., Sutin, N., Electron transfer reactions in condensed phases, *Annu. Rev. Phys. Chem.*, 1984, 35: 437.

11 Newton, M. D., Formalisms for electron-exchange kinetics in aqueous solution and the role of *ab initio* techniques in their implementation, *Int. J. Quantum Chem. Quantum Chem. Symp.*, 1980, 14: 263.